PHYSICAL REVIEW B **80**, 081304(R) (2009)

Impacts of structural asymmetry on the magnetic response of excitons and biexcitons in single self-assembled In(Ga)As quantum rings

Ta-Chun Lin,[1] Chia-Hsien Lin,[2] Hong-Shi Ling,[1] Ying-Jhe Fu,[1] Wen-Hao Chang,[2] Sheng-Di Lin,[1] and Chien-Ping Lee[1]
[1]*Department of Electronic Engineering, National Chiao Tung University, Hsinchu 300, Taiwan*
[2]*Department of Electrophysics, National Chiao Tung University, Hsinchu 300, Taiwan*
(Received 25 May 2009; revised manuscript received 20 July 2009; published 12 August 2009)

The diamagnetic shifts of neutral excitons and biexcitons confined in single self-assembled In(Ga)As/GaAs quantum rings are investigated. Unlike quantum dots, quantum rings reveal a considerably large biexciton diamagnetic shift, about two times larger than that of single excitons. Based on model calculations, we found that the inherent structural asymmetry and imperfection, combined with the interparticle Coulomb interactions, is the fundamental cause of the more extended biexciton wave function in the quantum rings. The exciton wave function tends to be localized in one of the potential valleys induced by structural imperfections of the quantum ring due to the strong localization of hole and the electron-hole Coulomb attraction, resembling the behavior in single dots. Our results suggest that the phase coherence of neutral excitons in quantum rings will be smeared out by such wave function localizations.

DOI: 10.1103/PhysRevB.80.081304 PACS number(s): 78.67.Hc, 73.21.La

Charged particles confined to a nanoscopic quantum ring (QR) are expected to show unique magnetic responses, i.e., the well-known Aharanov-Bohm (AB) effect, due to the quantum interference of the carrier's wave function in the ring-shaped geometry. Experimental evidence of such a purely quantum mechanical effect has been observed in metallic and semiconductor mesoscopic rings[1–4] and recently in nanoscopic QRs.[5–7] On the other hand, the exciton properties in ringlike nanostructures also gained a lot of interest recently. Because an exciton is a charge-neutral composite, the AB effect is not expected to occur unless the electron and hole can propagate coherently in different trajectories with a nonzero electric dipole moment.[8] Such a case appears naturally in type-II quantum dot (QD) systems,[9,10] where the electron and hole are spatially separated, resembling the behavior of single charges. However, for nanoscopic rings, such as InGaAs self-assembled QRs formed via partial capping of InAs QDs and subsequent annealing,[11,12] it is still an open question whether the excitonic AB effect can be observed when both the electron and hole are confined in the rings. In fact, this issue is further complicated by the inherent structural asymmetry and imperfections presented inevitably in self-assembled QRs. Although it has been demonstrated both experimentally and theoretical that the phase coherence of electron wave function in self-assembled QRs could survive,[7] the impacts of inherent structural asymmetry and imperfection on the magnetic response of neutral excitonic species, such as excitons (X) and biexcitons (XX) with the presence of Coulomb interactions, have yet to be investigated.

In this Rapid Communication, we report the diamagnetic response of X and XX in single self-assembled QRs. Unlike single QDs, the XX confined in single QRs shows a considerably larger diamagnetic coefficient than the X. Guided by numerical model calculations, we found that the inherent structural asymmetry and imperfection, combined with the interparticle Coulomb interactions, play a crucial role in the distribution of X and XX wave function in self-assembled QRs. Our results suggest that the phase coherence of neutral excitons in QRs will be smeared out by the wave function localization due to the structural asymmetry and imperfections.

The InAs QRs were fabricated by Varian Gen-II molecular-beam epitaxy on a GaAs (001) substrate. Low density QDs were first grown by depositing two monolayers of InAs at 520 °C as QR precursors. The substrate temperature was then lowered to 500 °C. A thin GaAs layer of 1.7 nm was deposited to cover the QD sidewalls, and a 50 s growth interruption was performed for a dewetting process which expels the indium atoms from the center of the QDs to move outwards for the QR formation. The detail of the growth can be found in Ref. 12. Surface topography of uncapped QRs has been investigated by atomic force microscopy. The area density of surface QRs is estimated to be about 1×10^7 cm^{-2}. As shown in Fig. 1, the surface QR has a rim diameter of 35 nm, a height of $\sim$1.3 nm, and a center dip of about 2 nm. The realistic dimension of the embedded QRs is expected to be much smaller.[13] We also found that the QR is anisotropic; the rim of the surface QR is higher along.[1–10]

The single QR emissions were measured by a low-temperature microphotoluminescence (μ-PL) setup combined with a 6 T superconducting magnet. The PL was excited by a 633 nm He-Ne laser, dispersed by a 750 mm monochromator and detected by a silicon charge coupled device camera. An aluminum metal shadow mask with arrays of 300 nm diameter apertures were used to isolate single QR emissions. A comparison between the PL spectra for the QR ensemble and a single QR is displayed in Fig. 1(d). The QR ensemble shows an emission peak at 1329 meV with a line width of 26 meV due to size fluctuations. For the single QR, the spectrum is dominated by a sharp emission line near 1320 meV with a resolution limited line width of $\sim$50 μeV.

Figure 2 shows the PL spectra taken from a representative single QR under different excitation powers. Two emission lines associated with the recombination from exciton (X) and biexciton (XX) states can be observed, which have been identified according to linear and quadratic power depen-

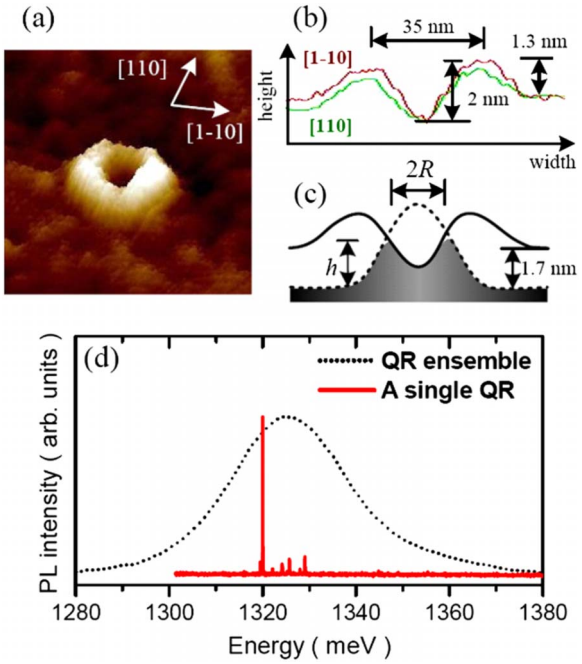

FIG. 1. (Color online) (a) The AFM image of the surface QR. (b) Topographical line scans along the [110] and the [1-10] directions. (c) A schematic for the surface QR profile (solid line), the precursor QD (dash line), and the indium-rich part of the embedded QR (gray part). (d) PL spectra taken from the QR ensemble and from a representative single QR.

dence of intensity as shown in the inset of Fig. 2. The same measurement has been performed on a total of seven QRs. The emission energies of X are in the range of 1320–1328 meV, while the biexciton binding energies (defined as $E_X - E_{XX}$) are varying from 0.2 to 0.7 meV for different QRs.

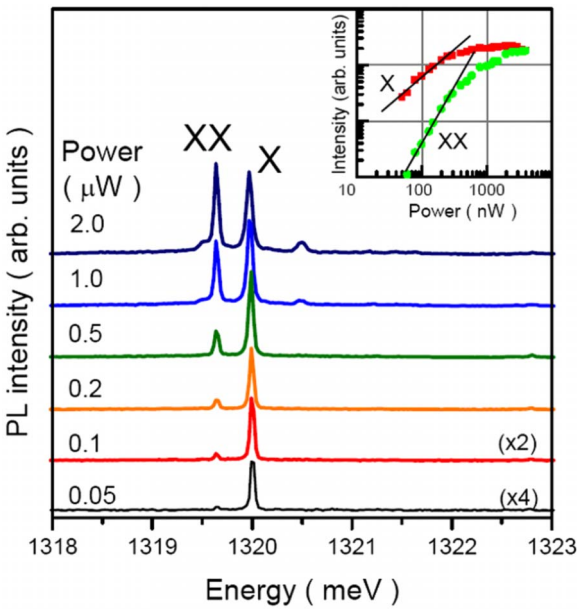

FIG. 2. (Color online) Power-dependent PL spectra of a single QR. The inset shows the integrated intensity of X and XX lines as a function excitation power.

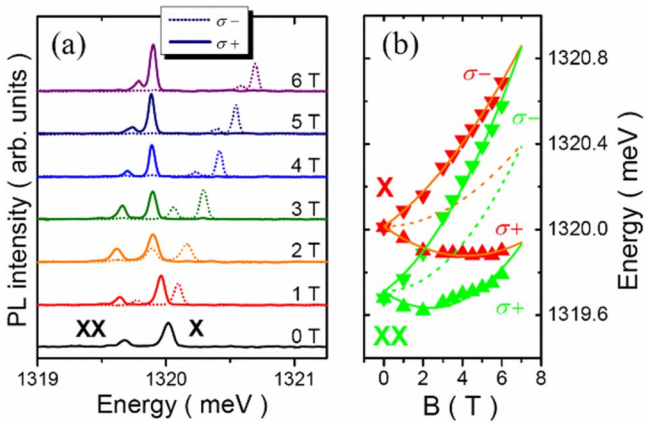

FIG. 3. (Color online) (a) Magneto-PL spectra for X and XX lines under different magnetic fields. (b) Emission peak energies of the X and XX Zeeman doublets as a function of magnetic field. Dash lines are quadratic fits to the averages of the Zeeman doublets.

When an external magnetic field is applied along the growth direction, each of X and XX lines splits into a cross circularly polarized doublet due to the spin Zeeman effect, as presented in Fig. 3. Because the exciton state is the final state of the spin-singlet biexciton state, both X and XX show an identical energy splitting of 131 μeV/T, corresponding to an excitonic g factor of $|g|=2.3$, a reasonable value for the InAs nanostructures embedded in GaAs matrix. The average energy of each Zeeman doublet shows a quadratic dependence on B, i.e., the diamagnetic shift, which can be fitted to γB^2, where γ is the diamagnetic coefficient. The average diamagnetic coefficient of X for all the investigated QRs is $\gamma_X=6.8$ μeV/T^2. Interestingly, we found that the XX shows a considerably larger diamagnetic coefficient with an average value of $\gamma_{XX}=14.8$ μeV/T^2, which is more than the double of the γ_X value.

The diamagnetic coefficient is proportional to the area of the excitonic wave function. Our results suggest that the XX wave function is more extended than that of X in a QR. This is different from the case of QDs,[15–18] where the diamagnetic response of XX is usually similar to, or somewhat smaller than, that of X due to the different spatial extents of the electron and hole wave functions and their responses to the applied B.

Here we argue that the more sensitive diamagnetic response of XX is a consequence of the fact that self-assembled QRs do not have perfect azimuthal symmetry. It has been reported that the structure of buried self-assembled QRs shows an asymmetric craterlike shape, with a diameter substantially smaller than the ring-shaped islands on the surface of uncapped QR structures. In addition, due to the preferential out diffusion of dot material along the[1–10] direction, the embedded rim height is higher along the [110] direction, resulting in two separate potential valleys along the [110] direction,[14] resembling a pair of connected QDs. The lack of rotational symmetry in the potential of embedded QRs is expected to have significant impacts on the diamagnetic responses of X and XX. For a neutral X, the height variation strongly localizes the hole inside one of the potential valleys due to the large effective mass. Consequently, the electron

will be bound to the same valley by the electron-hole Coulomb attraction. This means that the wave-function extent of X is determined mainly by the confinement of the potential valley and the Coulomb interaction. Therefore, the diamagnetic response of X is similar to an elliptic QD.

For a neutral XX confined in the QR, the two holes may be separately localized in different valleys due to the strong hole-hole Coulomb repulsion and the negligible coupling of hole states between the two valleys. Due to the Coulomb attractions of the two separately localized holes, the electron wave functions of XX are more likely to spread over the two valleys and become more extended than that of X. Unlike X, the wave-function extent XX is determined mainly by the diameter of the embedded QRs.

In order to further attest our assertions, we performed calculations of the X and XX states in our QRs based on structural information obtained from our atomic force microscopy topography and the proposed shape of embedded QRs reported in Ref. 13. A one-band effective mass Hamiltonian was used to calculate the single-particle states. The Coulomb interaction between the electron and hole was then treated self-consistently. According to Ref. 14, we model the QR as a nanoscale crater with an azimuthal asymmetric potential $V_H(\rho,\varphi)$ deduced from the z-axis quantization energy variation arising from the height anisotropy. The potential can be further simplified to $V_H(\rho,\varphi)=V_0(\rho)\cos 2\varphi$, where $V_0(\rho)$ is proportional to the height anisotropy factor ξ_h. Other parameters are listed in Ref. 19. Figures 4(b) and 4(c) depict the QR height profile and the corresponding radial potential $V_0(\rho)$ for the electron for a rim radius of $R=7$ nm, an average rim height of $h_M=2.5$ nm, and an anisotropy factor of $\xi_h=0.15$. The corresponding maximum V_0 is 19.5 and 9.8 meV at the rim for the electron and hole, respectively. The calculated electron wave functions for the lowest energy states of X and XX are plotted in Figs. 4(d) and 4(e), respectively. It can be seen that X is well confined in one side of the QR with a less extended wave function.[21] By contrast, the electron wave function of XX spreads over both sides of the QR. The diamagnetic response of X and XX can be further calculated by superimposing a magnetic confining potential to the QR potential. By fitting the calculated energy shift to the quadratic energy dependence γB^2 as depicted in Fig. 4(f), the diamagnetic coefficients of X and XX are found to be $\gamma_X=10.7$ μeV/T^2 and $\gamma_{XX}=23.0$ μeV/T^2, respectively. Although the model QR shape may be different from the actual shape of our QRs, our simulations demonstrate unambiguously that the asymmetric potential indeed impacts the diamagnetic response of X and XX, which agrees very well with our experimental finding.

In brief, the diamagnetic responses of excitons and biexcitons confined in single self-assembled QRs have been investigated. Unlike single QDs, the biexciton confined in single QRs shows a considerably larger diamagnetic coefficient than the exciton, implying the more extended biexciton wave functions in the ring. The lack of perfect rotational symmetry in the potential of embedded QRs due to the inherent structural asymmetry is the fundamental cause of the more extended biexciton wave function. The strongly localized holes in potential valleys of QRs leads to a localized exciton wave function due to the electron-hole Coulomb attraction, while makes the biexciton wave function being able to spread over the ring due to the hole-hole Coulomb repulsion. In other words, the Coulomb interactions combined with the reduced azimuthal symmetry caused by inherent structural imperfection could destroy any of the expected magnetic response that relies on the rotational symmetry of exciton and biexciton wave functions confined in self-assembled QRs.

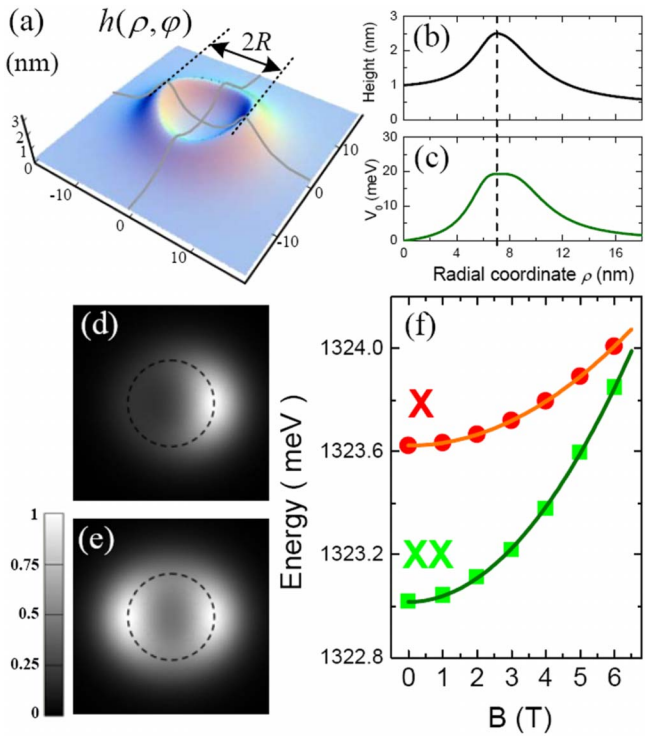

FIG. 4. (Color online) (a) A schematic for the QR geometry with an anisotropy factor $\xi_h=0.15$ used in our model calculations. (b) and (c) are the height profile $h(\rho)$ and the electron radial potential $V_0(\rho)$ of the model QR. (d) and (e) are the calculated electron wave functions of the lowest X and XX states. The dash circle represents the rim diameter of 14 nm. (f) The emission energies of X and XX as a function of B. γ_X and γ_{XX} are found to be 10.7 μeV/T^2 and 23.0 μeV/T^2 by fitting to $E=\gamma B^2$.

We acknowledge the support from the National Science Council under Contracts No. NSC97-2120-M-009-002, No. NSC97-2120-M-009-004, No. NSC97-2112-M-009-012, and National Nano Device Laboratories.

[1] L. P. Lévy, G. Dolan, J. Dunsmuir, and H. Bouchiat, Phys. Rev. Lett. **64**, 2074 (1990).
[2] V. Chandrasekhar, R. A. Webb, M. J. Brady, M. B. Ketchen, W. J. Gallagher, and A. Kleinsasser, Phys. Rev. Lett. **67**, 3578 (1991).
[3] D. Mailly, C. Chapelier, and A. Benoit, Phys. Rev. Lett. **70**, 2020 (1993).
[4] A. Fuhrer, S. Luscher, T. Ihn, T. Heinzel, K. Ensslin, W. Wegscheider, and M. Bichler, Nature (London) **413**, 822 (2001).
[5] A. Lorke, R. J. Luyken, A. O. Govorov, J. P. Kotthaus, J. M. García, and P. M. Petroff, Phys. Rev. Lett. **84**, 2223 (2000).
[6] M. Bayer, M. Korkusinski, P. Hawrylak, T. Gutbrod, M. Michel, and A. Forchel, Phys. Rev. Lett. **90**, 186801 (2003).
[7] N. A. J. M. Kleemans, I. M. A. Bominaar-Silkens, V. M. Fomin, V. N. Gladilin, D. Granados, A. G. Taboada, J. M. García, P. Offermans, U. Zeitler, P. C. M. Christianen, J. C. Maan, J. T. Devreese, and P. M. Koenraad, Phys. Rev. Lett. **99**, 146808 (2007).
[8] A. O. Govorov, S. E. Ulloa, K. Karrai, and R. J. Warburton, Phys. Rev. B **66**, 081309(R) (2002).
[9] E. Ribeiro, A. O. Govorov, W. Carvalho, Jr., and G. Medeiros-Ribeiro, Phys. Rev. Lett. **92**, 126402 (2004).
[10] I. R. Sellers, V. R. Whiteside, I. L. Kuskovsky, A. O. Govorov, and B. D. McCombe, Phys. Rev. Lett. **100**, 136405 (2008).
[11] D. Granados and J. M. García, Appl. Phys. Lett. **82**, 2401 (2003).
[12] H. S. Ling and C. P. Lee, J. Appl. Phys. **102**, 024314 (2007).
[13] P. Offermans P. M. Koenraad, J. H. Wolter, D. Granados, J. M. García, V. M. Fomin, V. N. Gladilin, and J. T. Devreese, Appl. Phys. Lett. **87**, 131902 (2005).
[14] V. M. Fomin, V. N. Gladilin, S. N. Klimin, J. T. Devreese, N. A. J. M. Kleemans, and P. M. Koenraad, Phys. Rev. B **76**, 235320 (2007).
[15] A. Kuther, M. Bayer, A. Forchel, A. Gorbunov, V. B. Timofeev, F. Schäfer, and J. P. Reithmaier, Phys. Rev. B **58**, R7508 (1998).
[16] A. Babinski, S. Awirothananon, J. Lapointe, Z. Wasilewski, S. Raymond, and M. Potemski, Physica E **26**, 190 (2005).
[17] R. J. Young, R. M. Stevenson, A. J. Shields, P. Atkinson, K. Cooper, D. A. Ritchie, K. M. Groom, A. I. Tartakovskii, and M. S. Skolnick, Phys. Rev. B **72**, 113305 (2005).
[18] M. F. Tsai, H. Lin, C. H. Lin, S. D. Lin, S. Y. Wang, M. C. Lo, S. J. Cheng, M. C. Lee, and W. H. Chang, Phys. Rev. Lett. **101**, 267402 (2008).
[19] The shape of QR is a crater with the height as a function of the radial coordinate ρ,

$$h(\rho) = h_0 + \frac{(h_M - h_0) \cdot (1 - (\rho/R - 1))^2}{[(\rho - R)/r_0]^2 + 1}, \quad \rho \leq R,$$

$$h(\rho) = h_\infty + \frac{h_M - h_\infty}{[(\rho - R)/r_\infty]^2 + 1}, \quad \rho > R \quad \text{(Refs. 13 and 14)}.$$

Here we model the QR with $R=7$ nm, $h_M=2.5$ nm, $h_0=1$ nm, $h_\infty=0.4$ nm, $r_0=2$ nm, and $r_\infty=3.5$ nm. The band offset of conduction (valence) band is 300 meV (180 meV) from the strained $In_{0.7}Ga_{0.3}As/GaAs$ QDs (Ref. 20). The effective mass of electron (hole) is 0.067 m_0 (0.5 m_0).
[20] C. E. Pryor and M.-E. Pistol, Phys. Rev. B **72**, 205311 (2005).
[21] For the two equivalent potential valleys in a QR, it may be expected that the exciton wave function is distributed symmetrically in both valleys. However, the calculation reveals that the lowest energy state is the localized exciton in one valley (i.e., either of the two) due to its stronger e-h Coulomb interaction. In other words, the exciton Bohr radius (about 11 nm for InAs QR) is slightly smaller than the ring diameter, which concentrates the exciton wave function into one side of the QR.